

## STUDY OF VITREOUS SILICA SINTERING BY SPARK PLASMA (SPS)

**Bruno Barazani, bruno.bara@usp.br**

**Delson Torikai, delson.torikai@poli.usp.br**

University of São Paulo, Mechatronics Department. Av. Prof. Mello Moraes, 2231. CEP: 05508-030 – São Paulo – SP.

**Carlos Kenichi Suzuki, suzuki@fem.unicamp.br**

State University of Campinas. Av. Mendeleev, 200. CEP. 13083-860 – Campinas – SP

**Abstract.** Spark Plasma sintering presents some different processing novelties concerning conventional sintering methods. Lower processing time and temperature and the high purity of the final specimens are some of them. The technique is characterized by the application of high electric current pulses, which causes the heating associated with the uniaxial compression of the sample. The quickness of the process allows the control of grain growth and keeping the powders distribution into the mold during the sintering, enabling the fabrication of graded and nano-structured materials. A great diversity of vitreous silica ( $\text{SiO}_2$ ) properties can be obtained by changing the fabrication conditions and by specific doping. This, and other features, makes vitreous silica one of the main materials used in micro fabrication process, optical devices - as filters, special windows and lenses - lithography masks, optoelectronics materials, fiber optics, optical amplifiers and others. Our aim is to investigate the fabrication of different types of pure vitreous silica by the SPS process. Three different raw materials of silica were used in the experiments: i) crystalline silica powder (alpha quartz) with average particle size of 100  $\mu\text{m}$ ; ii) sol-gel amorphous silica powder with the same dimensions; iii) aerosol-flame processed nanopowder of vitreous silica with particle size between 30 and 200 nm. The raw materials were inserted individually into the cylindrical graphite die with inner diameter of 20 mm which was placed in the sintering chamber - operated in vacuum atmosphere - of the equipment. Temperature, uniaxial compression, axial shrinkage of the sample and vacuum pressure of the chamber were controlled and/or monitored continuously all along the sintering process. Density measurements based on the Archimedes method using an analytical balance and X-ray diffractions with a  $\theta$ - $2\theta$  scan were performed on the samples produced. Transparent vitreous silicas were obtained from the three types of raw materials independently processed. For the crystalline powder, the material was obtained with heating rates of 60 and 140°C/min. with maximum temperatures of 1450 and 1600°C, respectively. For the sol-gel amorphous powder, and nanopowder, heating rates between 40 and 100°C/min and final temperature of 1225°C was enough to get dense and transparent material. X-ray diffraction and density measurements showed completely amorphous silica, with average density of 2.204 g/cm<sup>3</sup>. Small variation in the density data analysis also allowed identifying the presence of bubbles or pores in the structure of some specimens.

**Keywords:** Spark Plasma Sintering, Vitreous Silica, Sol-gel silica, Nanopowder.

### 1. INTRODUCTION

In the sintering process, fine particles of certain material bond themselves creating a unique solid to decrease their free energy. In this process, the raw material is heated until it reaches the activation energy of mass transport phenomena, i.e., surface and grain boundary diffusion (Rahaman, 2008). The high temperature and usually long treatment time increases the average grain size as it reduces the total energy of grain boundaries (Porter *et al*, 2009). However, for many industrial applications, it is desired to obtain high density materials with small grain size since these features provide important properties to the material.

The conventional sintering method - without application of pressure on the sample - is widely used because of its economical feasibility, even though it allows the grain growth and limits the final density of the solid (Rahaman, 2008). Other methods such as HP (hot pressing) and HIP (hot isostatic pressing), which apply external pressure on the particles result in higher density materials, since the compression induces densification mechanisms such as grain boundary diffusion in polycrystalline materials. In the case of amorphous particles, the mass transport occurs by viscous flow (Rahaman, 2008).

Silica or  $\text{SiO}_2$  is a chemical compound easily found in natural soils and it can present a variety of crystalline forms, such as quartz, cristobalite, and others (Sosman, 1967). However, it is in the amorphous solidified state that this material is called vitreous silica or fused silica and presents important applications in different sectors of the advanced technological industry as in the production of optical fibers, sensors (Yeh, 1990) and amplifiers (Prמוד *et al*, 2006), in the fabrication of crucibles for silicon crystal growth (Huang *et al*, 2005), special lens (Mizoshiri *et al*, 2008), beam splitters (Feng *et al*, 2009), microlithography applications (HERAEUS, 2011) and other functions such as thermal and electrical insulators.

The aim of this study is to investigate the fabrication of vitreous silica and composites of pure  $\text{SiO}_2$  starting from different raw materials of  $\text{SiO}_2$  by the Spark Plasma Sintering technique. Crystalline and amorphous powders of silica and nanopowder of amorphous silica were sintered separately and mixed and the results were analyzed by X-ray diffractions and density measurements

## 2. SPARK PLASMA SINTERING METHOD

Spark Plasma Sintering (SPS) is identified by the uniaxial pressure application on the raw material and by the heat generation from high electric current pulses applied directly on the sample and on the die (Tokita, 2000). This technique provides a great number of benefits and unique properties in relation to traditional sintering techniques due to the lower processing time and temperature (Tokita, 2000). The method is applied in the fabrication of functionally graded materials (FGMs), nano-structured materials, thermo-electrical materials, advanced ceramics and bio-materials, mainly because it permits the control of grain growth and improves mechanical properties. In the SPS technique, the high heating rates, typically between 100 e 600°C/min. brings the sample rapidly to large temperatures assisting densification mechanisms over non-densification mechanisms (Garay, 2010). The mechanical compression of the sample is another factor that accelerates the material densification in the SPS method (Rahaman, 2008). Due to these and to other features, SPS became a reference in the fabrication of FGMs and nanostructured materials by using nanopowders.

In the process, high electric current pulses are applied directly on the sample and on the graphite die. The temperature elevation occurs due to the Joule effect in the die, plungers, and eventually between the powder particles when they are in contact, and also by the sparks generated in the empty spaces between the particles of the raw material (Tokita, 2000 and Rahaman, 2008). The mechanical compression is performed by two vertical electrodes where the current pulses pass-through. The mold is set between the electrodes inside a chamber with controlled atmosphere. A programmable control unit and a high power electrical energy source are also provided. Figure 1 shows a scheme of the SPS system.

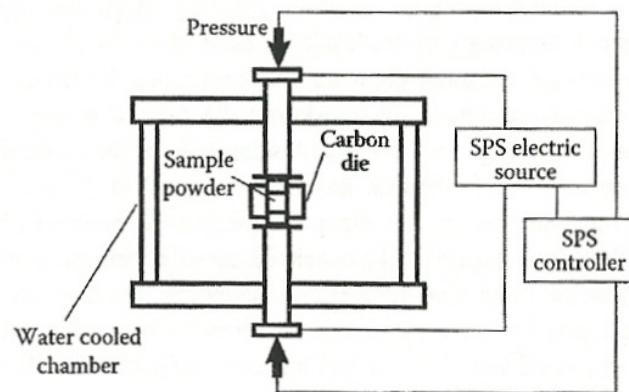


Figure 1. Simplified representation of the SPS system (Rahaman, 2008).

## 3. VITREOUS SILICA

Among the four principal polymorphic forms of silica - quartz, tridimite, cristobalite and liquid (Sosman, 1967) - only the liquid phase is considered amorphous and, therefore, does not present a pattern along the molecular structure as occurs with quartz (Fig. 2). Any crystalline form of silica can be converted into its amorphous phase if it is heated to a proper temperature and with proper heating rate. Quartz, for instance, becomes liquid at about 1400°C (Sosman, 1967). The liquid phase of silica, when cooled, originates vitreous silica that has the same amorphous structure, but characteristics of a solid. The passage from the liquid to the vitreous form occurs at the transition temperature “ $T_g$ ” (Callister, 2002) and as the two structures are amorphous, they differ only by their viscosities.

Vitreous silica is a material of many applications in the industry since it has peculiar properties such as low thermal expansion, low thermal conductivity, high chemical durability, high temperature stability and high optical transparency in a wide range of the light spectrum (Bansal and Doremus, 1986).

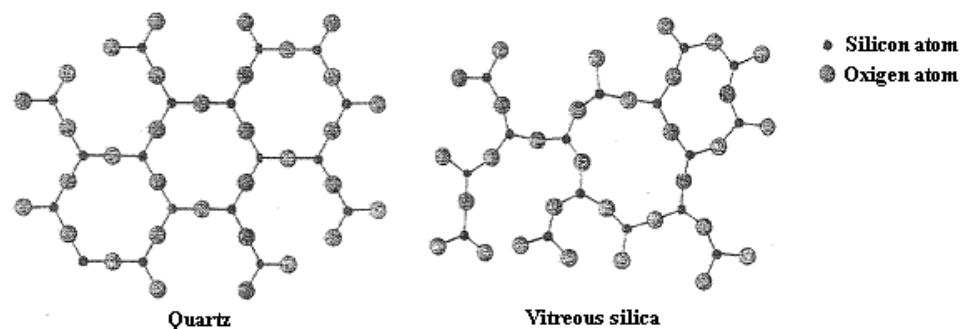


Figure 2. Quartz molecular structure compared with that of fused silica (Callister, 2002).

As an example of application, SiO<sub>2</sub> is used for the production of optical fibers due to its optical transparency, mechanical resistance and its dielectric and refractory properties. Generally, the core of the fiber is composed of glass doped with other oxides such as GeO<sub>2</sub> e TiO<sub>2</sub>, while the cladding only contains highly pure vitreous SiO<sub>2</sub> (Yeh, 1990).

#### 4. SINTERING OF SILICA

Vitreous silica is obtained by different methods (Bruckner, 1970) that can induce different glass properties (Kikuchi *et al*, 1997). Sintering is one of the possible processes used for this purpose, starting from crystalline or amorphous silica powders.

Yong-Taeg *et al*, 2002, concluded that the optimum temperature to reach dense vitreous silica by sintering pre-compacted bodies of amorphous powder – with average particle size of 0.4 μm - was higher than 1400°C in a high vacuum atmosphere (10<sup>-4</sup> Pa) and with holding time of around 17 minutes.

Fused silica was also obtained from crystalline powder (alpha-quartz with 70 μm of average size) by the SPS technique (Koide *et al*, 2002), in which vitreous compacts were obtained with a heating rate of 50°C/min. and final temperatures between 1500 and 1600°C, without holding time, but applying a mechanical compression of 20 MPa on the raw material.

In another study (Cardoso and Abreu, 1999), the mixture of alpha-quartz powders with pyrogenic silica (amorphous nanopowder) was sintered in an electric furnace at 1550°C for one hour using a heating rate of 5°C/min. When processed separately, both resulting samples presented cristobalite as the only crystalline phase, while the sintering of the crystal powder with additions of more than 10% of pyrogenic silica resulted in the presence of cristobalite and alpha-quartz crystals in the final sample.

#### 5. MATERIALS AND METHOD

##### 5.1. Raw materials

Table 1 describes the characteristics of high purity raw materials of silica used in this study.

Table 1. Characteristics of the powders used in the experiments.

Crystalline structure	Particle size	Obtainment process	Supplier
alpha-quartz	~ 100 μm	quartz chips powdering and purification	Kyushu Ceramics
amorphous	~ 100 μm	Sol-gel process	Mitsubishi Kasei Co.
amorphous	30 to 200 nm	Vapor-phase axial deposition	LIQC-Unicamp

##### 5.2. Preparation of the mold and Sintering

The powders were poured, separated or mixed, in a graphite die of 20 mm of inner diameter. Two graphite plungers apply the axial compression to the sample. The mechanical compression applied during the sintering was around 2 KN for every experiment and heating rates between 40 and 150°C/min were used. The temperature was measured by an optical pyrometer at the external surface of the mold. The temperature and compression force were controlled by a program and the axial contraction of the sample - vertical displacement of the plunger during densification - and vacuum pressure of the chamber were monitored all along whole process. All the process parameters were visualized in real time in a monitor connected to the equipment.

The same temperature routine program was used for the sintering of mixed samples, with different proportions of crystalline and amorphous powders as specified in Tab. 2.

Table 2. Mass proportions of crystalline and amorphous powders used in the mixture of raw materials.

	Crystalline powder mass (g)	Amorphous powder mass (g)	Total mass (g)	Amount of crystalline powder (%)	Amount of amorphous powder (%)
Mixture 1	2.732	3.040	5.772	47	53
Mixture 2	1.724	3.994	5.718	30	70

##### 5.3. Density measurement

The density measurements of the sintered samples were performed using the Archimedes principle with the aid of an analytical weight meter. The mass of the water displaced by the sample was measured, as suggests the concept of buoyant force. Knowing the water density at the temperature in which the measurement was performed, the sample density ( $d_s$ ) was calculated with good precision through Eq. (1).

$$d_s = m_s \cdot d_w / m_{wd}$$

(1)

Where ' $m_s$ ' is the sample mass, ' $d_w$ ' is the water density and ' $m_{wd}$ ' is the water displaced mass. The Archimedes method allows measuring the density of bodies with regular and irregular surfaces.

#### 5.4. X-Ray diffraction

X-ray analyses conducted at the Laboratory of Integrated Quartz Cycle from the University of Campinas - Unicamp - were performed on some of the samples. The diffractometer used a  $\theta$ - $2\theta$  configuration and the reflection intensity was measured at the interval  $10^\circ < 2\theta < 65^\circ$ , using  $\text{CuK}_\alpha$  radiation.

### 6. RESULTS AND DISCUSSIONS

#### 6.1. Raw materials sintered separately

The three types of powders used were sintered individually to obtain transparent vitreous silica free of bubbles. Table 3 shows some sintering process conditions, axial contraction during sintering, and density measurements.

Table 3. Processing parameters for different raw materials of  $\text{SiO}_2$  sintered independently by the SPS technique.

Type of powder	Mass (g)	Heating rate (°C/min.)	Final temperature (°C)	Holding time (min.)	Contraction (mm)	Density (g/cm <sup>3</sup> )
Crystalline	5.7	60 (all process)	1455	2	1.2	2.216
Crystalline	5.7	140 (after 750°C)	1610	0	1.3	2.200
Nano amorphous	2.5	40 (until 840°C), 100 (after 840°C)	1225	4	7.5	2.198
Nano amorphous	2.5	150 (after 600°C)	1360	0	8.5	2.165
Amorphous	5.7	40 (until 840°C), 100 (after 840°C)	1230	4	3.5	2.203

The transparent compacts obtained from the crystalline powder with greater heating rate (140°C/min) demanded a high final temperature up to 1610°C. For the heating rate of 60°C/min, the final temperature of 1455°C was enough to get completely amorphous material (Fig. 5). Although high heating rates save processing time, it is necessary to increase the maximum temperature so as to make up for the slow heat diffusion at the silica grains.



Figure 5. Sample obtained from the sintering of crystalline powder with 60°C/min. of heating rate.

The production of transparent fused silica free from bubbles from the amorphous nanopowder (Fig. 6a) was only possible by lowering the heating rate (40°C/min.) for temperatures below ~840°C. At about 700°C, a large liberation of gas by the silica soot was observed, which remains in the open pores generating bubbles when high heating rates are used. When lower heating rates are used - up to 840°C - in order to increase the action time of the vacuum pump to remove the gases before the beginning of the densification, bubble-free silica is obtained. For temperatures higher than 840°C, higher heating rates up to 150°C/min. may be used without generating bubbles. The micro-bubbles caused a decrease in the value of the compacts density (Table 3) and also made it completely opaque (Fig. 6b).

The final temperature used to obtain vitreous silica from the amorphous powder (Fig. 7) was close to that of the nanopowder (~1220°C), since the two raw materials have amorphous structure. In the case of the crystalline powder, it was necessary to reach the fusion temperature of alpha-quartz, at temperatures higher than 1400°C.



Figure 6. Transparent fused silica obtained from amorphous nanopowder (a). Milky glass due to numerous micro-bubbles (b).



Figure 7. Compact obtained starting from amorphous SiO<sub>2</sub> powder.

The contractions during densification were larger for the nanopowder as compared to the other raw materials with particle size of the order of micrometers, as shown in Tab. 3. This occurs because powders with dimensions lower than 1  $\mu\text{m}$  agglomerates easily (Rahaman, 2008) making their compaction difficult before heating. In this case, the volumetric contraction is much larger during sintering, as there is more porosity to be closed.

All of the transparent vitreous samples presented densities near 2.200  $\text{g}/\text{cm}^3$ , the same value found in the literature for pure silica glass. X-ray analyses indicated the amorphous structure of these specimens since there were not peaks of reflection which are typical of crystalline formations (Fig. 8).

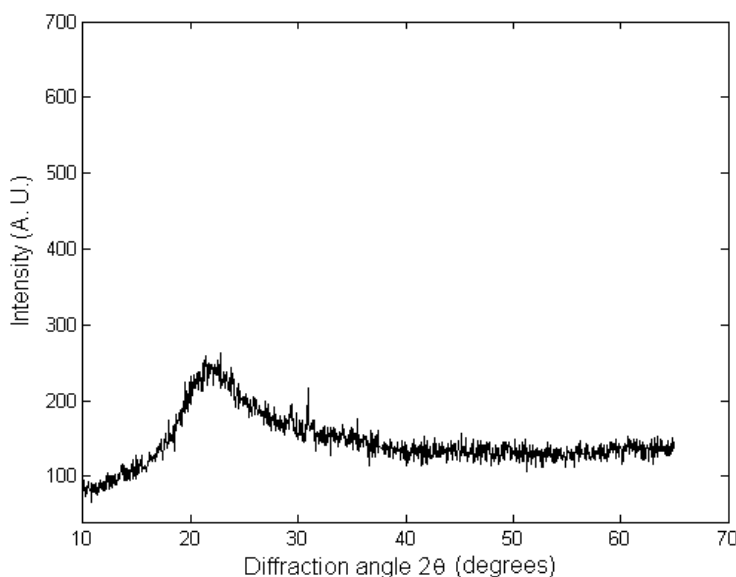


Figure 8. Diffractogram of a vitreous sample taken from crystalline powder.

The completed sintering cycle used in the experiment had the maximum time of 30 minutes, which is very short if compared to conventional sintering processing times.

## 6.2. Mixtures of SiO<sub>2</sub> powders sintering

A preliminary study, sintering different mixtures of amorphous and crystalline silica powders, showed the possibility to obtain dense glass-ceramic composed only by high-purity silica (see Fig. 9). For such a process, the final sintering temperature used was up to 1350°C, which is greater than the sintering temperature of the amorphous powder, but lower than the fusion temperature of the crystalline powder. The X-ray diffractograms of these samples (Fig. 10) showed only diffraction peaks of alpha-quartz crystal.



Figure 9. Silica glass-ceramic composed of Amorphous SiO<sub>2</sub> matrix reinforced with alpha-quartz particles.

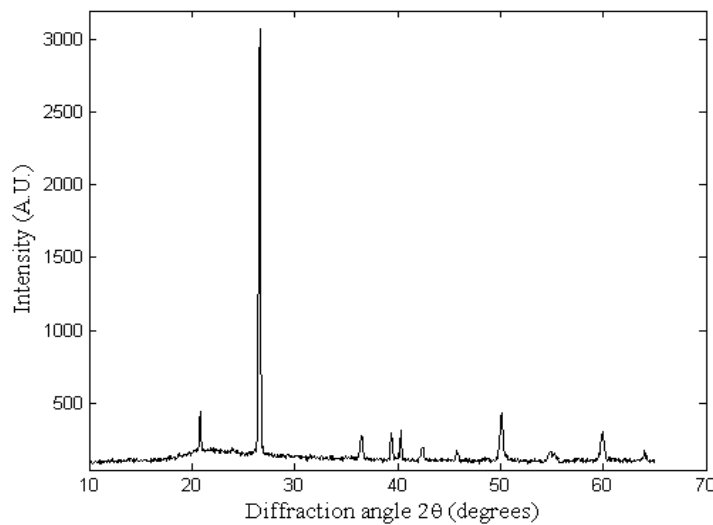


Figure 10. Diffractogram of one of the silica glass-ceramic obtained by mixing amorphous and crystalline powders.

The graphic of Fig. 11 shows the temperature curve of these experiments and how the axial contractions changes with time for different mixtures of powders. As the densification occurs only for the amorphous powder, it explains the larger axial contraction of the mixture with greater amount of this powder. Table 4 presents the values of the silica glass-ceramics densities for the different powder ratios.

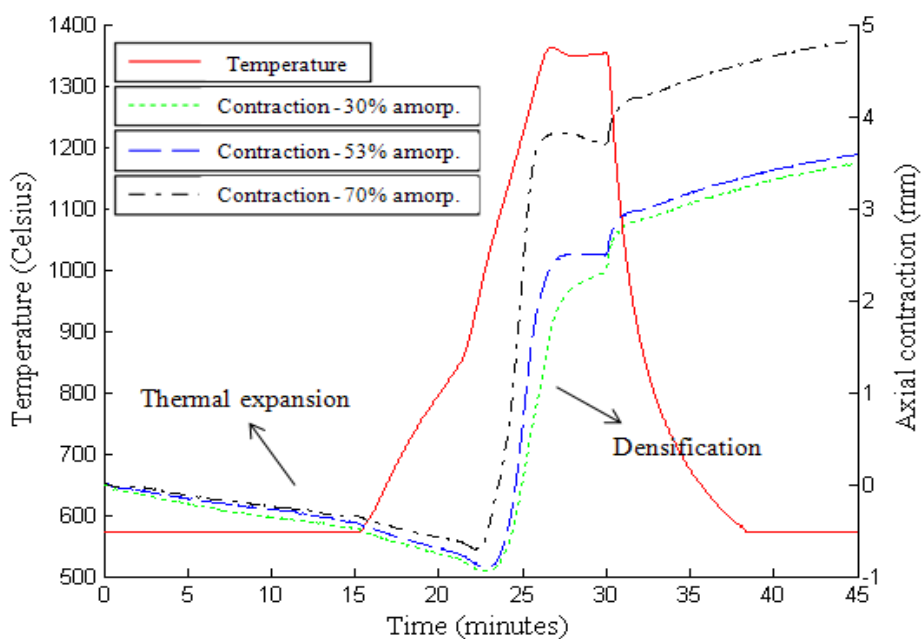


Figure 11. Axial contraction of the samples and temperature as a function of time.

Table 4. Densities of the pure silica glass ceramics fabricated.

Sample	Composition	Density (g/cm <sup>3</sup> )
1	53% amorphous e 47% Crystalline	2.33
2	70% amorphous e 30% Crystalline	2.30

The higher density of sample 1 compared with sample 2 agrees with the higher concentration of crystalline phase in the sample, as the density of alpha-quartz is about 2.60 g/cm<sup>3</sup> against 2.20 g/cm<sup>3</sup> of the vitreous silica.

## 7. CONCLUSIONS

Fused silica (vitreous SiO<sub>2</sub>) was produced by Spark Plasma Sintering from different raw materials of pure SiO<sub>2</sub> - powders with amorphous and crystalline structure with dimensions in the order of micrometers and amorphous nanopowders. All of the types of powders separately processed were converted into transparent vitreous monoliths of SiO<sub>2</sub> free from bubbles.

Temperatures around 1450°C were enough to fuse and to completely densify the crystalline powder for a heating rate of 60°C/min., while for a rate of 140°C/min. a final temperature up to 1600°C was required. Nanopowder and amorphous powder were compacted independently at temperatures around 1225°C. The reduction of the heating rate in the sintering of the nanopowder was necessary to increase the action time of the vacuum pump in removing the liberated gases from the raw material before the beginning of consolidation.

The fabrication of high pure silica glass-ceramics composed of vitreous silica reinforced with alpha-quartz particles was performed using the final temperature of 1350°C which is greater than the sintering temperature of the amorphous powder, but lower than the fusion temperature of the crystalline powder.

The density measurements indicated values of 2.20 g/cm<sup>3</sup> for the vitreous samples, and values of 2.30 g/cm<sup>3</sup> and 2.33 g/cm<sup>3</sup> for the specimens composed of crystalline and amorphous silica in the proportion of 30% crystal/70% amorphous and 47% crystal/53% amorphous, respectively.

X-ray diffraction confirms the amorphous structure of the fused silica produced and the presence of only alpha-quartz crystals in the glass-ceramic composite fabricated from the mixture of crystalline and amorphous powders.

## 8. ACKNOWLEDGEMENTS

The authors are grateful to Prof. Dr. Julio Adamowski for the use of SPS equipment. One of the authors, Bruno Barazani, thanks CAPES for the financial support of his study.

## 9. REFERENCES

- Bansal, N. P. and Doremus, R. H., 1986. "Handbook of Glass Properties". Ed. Academic Press, San Diego, United States, PP. 686.
- Brockner, R., 1970. "Properties and structure of vitreous silica". Journal of Non-Crystalline Solids, Vol. 5, pp. 123-175.
- Callister Jr, W. D., 2002. "Ciência e engenharia de materiais: uma introdução." Ed. Livros Técnicos e Científicos, Rio de Janeiro, Brazil, 589 p.
- Cardoso, A.V. and Abreu, W. M., 1999. "The sintering of v-SiO<sub>2</sub> and quartz" Journal of Non-Crystalline Solids, Vol 247, pp. 103-107
- Feng J., Zhou, C. Zheng, J., Cao, H., and Lv, P., 2009. "Design and fabrication of a polarization-independent two-port beam splitter". Applied Optics, Vol. 48, No. 29, pp. 5636-5641.
- Garay, J. E., 2010. "Current-Activated, Pressure-Assisted Densification of Materials" Annual Review Material Research, Vol 40, pp. 445-468.
- HERAEUS, 2011. "Suprasil® 501 ArF / 502 ArF". Heraeus Quarzglas. 03 Mar. 2011. <[http://optik.heraeus-quarzglas.de/en/productsapplications/productdetail\\_14592.aspx?psMarketId=1312&psApplicationId=762756](http://optik.heraeus-quarzglas.de/en/productsapplications/productdetail_14592.aspx?psMarketId=1312&psApplicationId=762756)>.
- Huang, X., Koh, S, Wu, K., Chen, M., Hoshikawa, T, Hoshikawa, K. and Uda, S., 2005 "Reaction at the interface between Si melt and a Ba-doped silica crucible". Journal of Crystal Growth, Vol. 277, pp. 154-161.
- Kikuchi, Y., Sudi, H. and Kuzuu, N., 1997. "OH content dependence of viscosity of Vitreous Silica". Journal of the Ceramic Society of Japan. Vol. 105[8], pp. 645-649.
- Koide, M., Takei, S., Sato, T. and Matusita, K., 2002. "Preparation of Silica Glass by Electric Current Method". Journal of the Ceramic Society of Japan, Vol. 110 [9], pp. 867-869.
- Mizoshiri, M., Nishiyama, H., Kawahara, T., Nishii, J., and Hirata, Y., 2008. "SiO<sub>2</sub>-Based Hybrid Diffractive-Refractive Lenses Fabricated by Femtosecond Laser-Assisted Micromachining". Applied Physics Express. No 1 pp. 127001-127001-3.
- Pramod R. W., Seongmin J., and Won-Taek H., 2006. "A Nd-YAG Laser-Pumped Tm-Doped Silica Glass Optical Fiber Amplifier at 840 nm". IEEE photonics technology letters, Vol. 18, No. 15, pp. 1651-1653.
- Porter, D. A., Easterling, K. E. and Sherif, M. Y. "Phase transformations in Metals and alloys" Ed. CRC Press, Boca Raton, United States, 500p.

Rahaman, M. N., 2008, "Sintering of Ceramics", Ed. CRC Press, Boca Raton, United States, 388p.

Sosman, R. B., 1967. "The phases of silica". Ed. Rutgers University Press New, Brunswick, United States, 388 p.

Tokita, M., 2000. "Mechanism of Spark Plasma Sintering". Proceedings of Powder Metallurgy World Congress".  
Kyoto, Japan, p.729-32.

Yeh, C., 1990. "Handbook oh Fiber Optics: Theory and Applications". Ed. Academic Press, San Diego, United States,  
382 p.

Yong-Taeg, O., Fujino, S. and Morinaga, K., 2002. "Fabrication of transparent silica glass by powder sintering."  
Science and Technology of Advanced Materials, Vol 3, pp. 297-301.

## **10. RESPONSIBILITY NOTICE**

The authors are the only responsible for the printed material included in this paper.